

# Treatment of Correlation Effects in Electron Momentum Density: Density Functional Theory and Beyond

B. Barbiellini and A. Bansil

*Department of Physics, Northeastern University, Boston, MA 02115 USA*

## Abstract

Recent high resolution Compton scattering experiments clearly reveal that there are fundamental limitations to the conventional local density approximation (LDA) based description of the ground state electron momentum density (EMD) in solids. In order to go beyond the framework of the density functional theory (DFT), we consider for the correlated system a BCS-like approach in which we start with a singlet pair wavefunction or a 'geminal' from which the many body wavefunction is then constructed by taking an antisymmetrized geminal product (AGP). A relatively simple practical implementation of the AGP method is developed where the one-particle orbitals are approximated by the Kohn-Sham solutions used in standard band computations, and the orbital-dependent BCS energy scale  $\Delta_i$  is determined through a readily computed exchange-type integral. The methodology is illustrated by considering EMD and Compton profiles in Li, Be and Al. It is found that in Li the present scheme predicts a substantial renormalization of the LDA result for the EMD; in Be, the computed correlation effect is *anisotropic*, while in Al, the deviations from the LDA are relatively small. These theoretical predictions are in qualitative accord with the corresponding experimental observations on Li, Be and Al, and indicate the potential of the AGP method for describing correlation effects on the EMD in wide classes of materials.

**Keywords:** Density Matrix, Electron-Electron Correlation, Natural Orbitals, Electron Momentum Density, Compton Profile.

## I. INTRODUCTION

Recent high resolution Compton scattering experiments on a number of materials clearly show that the EMD of the ground state is not described satisfactorily by the conventional LDA-based framework [1–11]. In Li, the size of the discontinuity  $Z_k$  in the EMD at the Fermi momentum  $p_F$  appears to be anomalously small<sup>1</sup> –nearly zero [1–4], and differs sharply from the values of 0.55 – 0.85 deduced via a variety of studies of the correlated homogeneous electron gas (HEG) stretching over last several decades [12–17]. In Be, comparisons between highly accurate computed and measured Compton spectra [7] indicate systematic discrepancies which are *anisotropic* and would be difficult to explain within the standard Lam-Platzman (LP) type correlation correction to the EMD [18–20] which is *isotropic* by construction. The EMD in Al, on the other hand, is adduced to be reasonably close to the LDA predictions [8–10]. Several attempts have been made to gain a theoretical handle on this problem [21–25]. The early optimism of a GW computation [21] in Li did not hold up to a later investigation [22,23]. Surprisingly, Quantum Monte-Carlo (QMC) studies of Si and Li [24,25] also do not reveal any substantial differences in the EMD with respect to the LDA predictions. It should be emphasized that a successful theory must not only explain what may be thought of as the "low" density case of monovalent Li, but also it must approach the LDA results correctly in the "high" density limit of trivalent Al in addition to explain the behavior of divalent Be.

In order to make progress, we observe first that the current GW and QMC computations in connection with the EMD assume that the fermionic correlation is not modified drastically by interactions and that an adiabatic path exists between the free and the interacting electron gas. The many body wavefunction underlying the GW and QMC work is built from Slater determinants of single-particle orbitals, with an implicit nodal structure and plasmon-type

---

<sup>1</sup>We will not concern ourselves here with possible complications in the interpretation of Compton data with regard to questions of background subtraction, failure of impulse approximation, etc.

physics of correlations [26] which is more or less similar to that of the LDA [27]. Bearing these considerations in mind, we have been motivated to examine other strategies, and here we propose a BCS-like approach for going beyond the framework of the DFT [28–33], wherein we start with singlet electron pairs—referred to as ‘geminals’ [34], and then combine these objects into an antisymmetrized product (AGP) to obtain the wavefunction of the many body system. Such an idea has been invoked previously, for example, in connection with liquid  $\text{He}^3$  [31] and in quantum chemistry calculations of molecules [30]. An application to the problem of the EMD in extended systems which is presented here has, to our knowledge, not been reported in the literature before. Notably, the AGP wavefunction in molecules typically yields only 40 – 50 % of the available correlation energy [30]. However, our main goal here is to develop a working scheme which can capture some of the essential physics of the EMD of the correlated electron gas, and not so much to obtain the total energy accurately. In this spirit, it is hoped that the AGP method can provide a useful tool for understanding the recent Compton spectra and the nature of the EMD over a wide range of electron densities.

An outline of this article is as follows. We start in Section II with a rigorous expression for the EMD,  $\rho(\mathbf{p})$ , in the correlated electron gas in terms of the eigenvalues and eigenfunctions of the one-particle density matrix  $\hat{\rho}(\mathbf{r}, \mathbf{r}')$  [35,36]. Section III discusses the conventional Lam-Platzman (LP) treatment [18–20] of correlations within the LDA which is based on the momentum density  $\rho_h(p)$  of the interacting HEG [12–17], including a useful parametrization of the more recent QMC data for  $\rho_h(p)$  [17]. Section IV takes up a description of the AGP wavefunction and the associated total energy functional [32]. A relatively simple practical implementation of the AGP scheme is discussed in Section V. The theory is illustrated by considering aspects of the EMD and Compton profiles in Li, Be and Al in Section VI. We emphasize that although these results indicate that the present method is promising, further work is necessary for confronting the AGP model quantitatively with experiments. Finally, Section VII summarizes the main results of this article.

## II. MOMENTUM DENSITY AND NATURAL ORBITALS

We start with the one-particle density matrix,  $\hat{\rho}(\mathbf{r}, \mathbf{r}')$ , which is defined in terms of the normalized N-particle wavefunction,  $\Psi$ , as

$$\hat{\rho}(\mathbf{r}, \mathbf{r}') = N \int d\xi \Psi^*(\mathbf{r}, \xi) \Psi(\mathbf{r}', \xi) , \quad (1)$$

where the integral extends over the coordinates of all other particles. The eigenfunctions and eigenvalues of  $\hat{\rho}$  define the *natural orbitals*,  $\psi_i$ , and the associated occupation numbers,  $n_i$  [35]. The density operator  $\hat{\rho}$  can then be expanded into projectors  $|\psi_i\rangle\langle\psi_i|$  via the spectral theorem:

$$\hat{\rho} = \sum_{i=1}^{\infty} n_i |\psi_i\rangle\langle\psi_i| . \quad (2)$$

If one requires the natural orbitals to possess the symmetry of the Hamiltonian, then they constitute a unique decomposition in an orthonormal basis set. Other basis sets for describing the many body wavefunction are often used, e.g. the *generalized overlap amplitudes* [36] which are linearly dependent. Any basis set can of course be related to the natural orbitals through an appropriate canonical transformation.

The EMD is defined as the momentum transform of the density matrix,

$$\rho(\mathbf{p}) = \frac{1}{8\pi^3} \int \int d^3\mathbf{r} d^3\mathbf{r}' \hat{\rho}(\mathbf{r}, \mathbf{r}') \exp(-i\mathbf{p} \cdot (\mathbf{r} - \mathbf{r}')) . \quad (3)$$

Note that, in general, the EMD involves off-diagonal elements of the real space density matrix. In terms of the natural orbitals  $\psi_i$ , however, the EMD can be cast in the simple form

$$\rho(\mathbf{p}) = \sum_i n_i | \langle \mathbf{p} | \psi_i \rangle |^2 , \quad (4)$$

where  $\langle \mathbf{p} | \psi_i \rangle$  is the momentum transform of  $\psi_i$ .

If the many body wavefunction is represented by a single determinant, which is true in the case of Hartree Fock or the DFT [37], then the density matrix is idempotent ( $\hat{\rho} = \hat{\rho}^2$ ) and reduces to a summation over the occupied spin-dependent orbitals  $\psi_i$ , i.e.

$$\hat{\rho}(\mathbf{r}, \mathbf{r}') = \sum_{i=1}^N \psi_i(\mathbf{r}) \psi_i^*(\mathbf{r}'). \quad (5)$$

The EMD in this *independent particle model* (IPM) is similar to the more general Eq. (2), except that the occupation numbers are now strictly 0 or 1 depending upon whether the state in question is empty or filled. Electron correlations, in effect, allow these occupied and empty IPM states to mix so that the occupation of states below the Fermi energy ( $E_F$ ) becomes less than 1, while that of states above  $E_F$  becomes non-zero.

One further point is noteworthy. In a periodic system, the electronic states are the Bloch states,  $\psi_{\mathbf{k}\mu}(\mathbf{r})$ , where  $\mu$  is the band index and  $\mathbf{k}$  is the crystal momentum which is restricted to the first Brillouin zone (BZ). The associated occupation numbers,  $n_i = N_\mu(\mathbf{k})$ , possess translational symmetry, i.e.

$$N_\mu(\mathbf{k}) = N_\mu(\mathbf{k} + \mathbf{G}_n), \quad (6)$$

with respect to the set of reciprocal lattice vectors  $\mathbf{G}_n$ .

### III. CORRELATION CORRECTION IN THE DENSITY FUNCTIONAL THEORY

As a consequence of the Hohenberg-Kohn theorem [27], the ground-state expectation value of any operator  $\hat{O}$  is a functional  $O[n(\mathbf{r})]$  of the electron density  $n(\mathbf{r})$ . It can be shown that [19]

$$O[n(\mathbf{r})] = O_0[n(\mathbf{r})] + \frac{d}{d\lambda} E_{xc}[n(\mathbf{r})](\lambda), \quad (7)$$

where  $O_0[n(\mathbf{r})]$  is the expectation value for a system of noninteracting fermions moving in the effective field involved in the Kohn-Sham formalism,  $E_{xc}$  is the exchange-correlation energy functional and  $\lambda$  is a scalar coupling parameter for the operator  $\hat{O}$ . The value obtained for the non-interacting case—given by the first term on the right side of Eq. (7), must be corrected by the second term. This so-called LP correction [18] provides a formal scheme for treating correlation effects in the interacting system within the DFT.

Insofar as the momentum density in extended systems is concerned, LDA is perhaps the most common implementation of the DFT. The relevant expression for the LP correction,  $\Delta\rho[n(\mathbf{r})](p)$ , is based on the treatment of  $E_{xc}$  in the HEG [19].

$$\Delta\rho[n(\mathbf{r})](p) = \int_{\text{WS}} [\rho_h(r_s(\mathbf{r}), p) - \rho_0(p)] n(\mathbf{r}) d^3\mathbf{r} . \quad (8)$$

Here, the integral extends over the Wigner-Seitz (WS) unit cell. The square brackets in the integrand give the difference between the momentum densities  $\rho_h$  and  $\rho_0$  of the interacting and non-interacting HEG, respectively, evaluated at the local density  $n(\mathbf{r})$  of the physical system given by the electron density parameter  $r_s(\mathbf{r})$ .

Despite the limitations of form (8) –a point to which we return below, this equation has been used extensively in the literature for evaluating the LP correction by using a variety of different results for the HEG starting with the work of Daniel and Vosko [12–17]. The most recent QMC data for  $\rho_h(p)$  however would be the most satisfactory to employ [17].

With this motivation, we provide a convenient formula for  $\rho_h(r_s, p)$  as a function of  $r_s$ , which we have obtained by parameterization of the QMC data [17]. For HEG of density  $n$

$$r_s = \left(\frac{3}{4\pi n}\right)^{1/3} . \quad (9)$$

We write QMC results for  $\rho_h(p)$  as

$$\rho_h(r_s, p) = \begin{cases} a(1) (1 - a(2) x^2), & \text{if } x \leq 1; \\ a(3) \exp(-a(4) (x - 1)) + T/x^8 & \text{otherwise,} \end{cases} \quad (10)$$

where  $x = p/p_F$  with  $p_F = (9/4\pi)^{1/3}/r_s$ , and  $a(1)$  through  $a(4)$  are  $r_s$ -dependent fitting parameters. Our form of  $\rho_h(r_s, p)$  differs somewhat from that given by Farid et al. [16], in that the tail in Eq. (10) is exponential while Ref. [16] uses a Gaussian tail. The coefficient  $T$  is given by Yasuhara and Kawazoe [38] as

$$T = \frac{4}{9} \left(\frac{\alpha r_s}{\pi}\right)^2 g(0) , \quad (11)$$

where  $\alpha = (4/9\pi)^{1/3}$  and

$$g(0) = \frac{64}{(8 + 5 r_s + 383/1200 r_s^2)^2} , \quad (12)$$

is the pair correlation function at  $r = 0$ , which has been obtained analytically by Overhauser [39]. Finally, we have fitted the coefficients  $a(1)$  through  $a(4)$  to the QMC data and obtained the following values.

$$\begin{aligned} a(1) &= 1 - .010 r_s, \\ a(2) &= 0.025 r_s, \\ a(3) &= 32/13 \delta, \\ a(4) &= 4, \end{aligned} \quad (13)$$

where  $\delta$

$$\delta = 1/3 - a(1) (1/3 - 1/5 a(2)) - \frac{T}{5} \quad (14)$$

has been chosen to satisfy the electron number sum rule. Fig. 1 shows that the QMC results parametrized here over the typical metallic range of densities ( $r_s$  varying between 2 and 5) differ significantly from those given by the early work of Lundqvist [13] parametrized by Cardwell and Cooper [20]; the original QMC data points lie indistinguishably close to the fitted solid curve of Fig. 1 and are not shown for simplicity.

#### IV. TREATMENT OF CORRELATION EFFECTS BEYOND THE DFT

The LP expression of Eq. (8) suffers from a number of limitations. Most importantly, this form only describes an *isotropic* redistribution of the EMD, even though the effect of correlations will in general be *anisotropic*. This also implies that the LP corrected EMD will possess a spurious feature at the free electron Fermi radius in all directions in the momentum space. Finally, the movement of spectral weight from below to above  $E_F$  in Eq. (8) is not very transparent in the sense that it is not associated directly with changes in the occupation numbers of various states, making it very difficult to impose reasonable physical conditions on the occupation numbers such as those of translational symmetry of Eq. (6).



Bearing these considerations in mind, and the fact that the QMC and GW results based on the LDA in Li [23,25] are not all that different from the LP correction and, therefore, would not explain the experimental EMD in Li, it is clear that there is need to go beyond the basic form of the Slater-Jastrow many-body wavefunction implicit in much of the QMC work given by

$$\Psi = F D^\uparrow D^\downarrow, \quad (15)$$

where the Jastrow factor  $F$  accounts for the plasmon zero modes [26] and  $D^\uparrow$  and  $D^\downarrow$  are Slater determinants for up and down spin electrons. To make a headway, we propose using a BCS-like many body wavefunction in which individual elements involve *singlet electron pairs*, rather than one-particle orbitals. The underlying nodal structure of such a many body wavefunction tends to minimize the effects of the exclusion principle [28]. As already noted, such an approach has been invoked in a variety of problems in the literature over the years [30–33], and here we are suggesting its use in connection with the treatment of momentum density in extended systems.

The starting point is a singlet pair wavefunction or the associated *generating geminal*  $\phi(\mathbf{r}_1 \uparrow, \mathbf{r}_2 \downarrow)$  [32,34], which can be expressed in a diagonal expansion of natural spin orbitals with undetermined coefficients  $g_i$ 's:

$$\phi(\mathbf{r}_1 \uparrow, \mathbf{r}_2 \downarrow) = \sum_i g_i \psi_i^*(\mathbf{r}_1) \psi_i(\mathbf{r}_2) [| \uparrow \rangle | \downarrow \rangle - | \downarrow \rangle | \uparrow \rangle]. \quad (16)$$

The many body wavefunction then is the AGP

$$\Psi = \hat{A} \left\{ \prod_{i=1}^{N/2} \phi(\mathbf{r}_i \uparrow, \mathbf{r}_j \downarrow) \right\}, \quad (17)$$

where  $\hat{A}$  is the antisymmetrization operator. The AGP belongs to the category of wavefunctions of *extreme type* [34]. <sup>2</sup> Eq. (17) can be cast into an  $N/2 \times N/2$  determinant

---

<sup>2</sup> Incidentally, if  $N$  is odd, the extreme type wavefunction is proportional to the antisymmetrized product of a one body orbital  $f$  and  $(N - 1)/2$  factors of  $\phi$ ;  $f$  must be strongly orthogonal to  $\phi$ , that is,  $\int f(\mathbf{r}_1) \phi(\mathbf{r}_1, \mathbf{r}_2) d^3 \mathbf{r}_1 = 0$  for all  $\mathbf{r}_2$  [34].

$$\Psi = \text{Det}|\phi(\mathbf{r}_i \uparrow, \mathbf{r}_j \downarrow)|. \quad (18)$$

The one-body wavefunctions  $\psi_i$  are the natural orbitals for not only the generating geminal  $\phi$ , but also for the AGP wavefunction  $\Psi$  [32]. For a two electron system, AGP is exact and equivalent to a configuration interaction calculation.

The  $\psi_i$ 's and  $g_i$ 's may be determined by minimizing the total energy functional. In extended systems the coefficients  $g_i$  are not particularly convenient, and it is more useful to introduce a new set of coefficients  $h_i$  to define a "Cooper pair" function given by:

$$C(\mathbf{r}_1 \uparrow, \mathbf{r}_2 \downarrow) = \sum_i h_i \psi_i^*(\mathbf{r}_1) \psi_i(\mathbf{r}_2) [| \uparrow \rangle | \downarrow \rangle - | \downarrow \rangle | \uparrow \rangle] \quad (19)$$

The non-Hartree-Fock-like term in the total energy can then be written as [32]

$$E[h_i, \psi_i] = E_{HF}[\hat{\rho}] + E_{BCS}[h_i, \psi_i] + O(1/N), \quad (20)$$

where  $E_{HF}$  is the Hartree Fock functional and  $E_{BCS}$  is a BCS-type functional [29,32] given by

$$E_{BCS} = \frac{1}{2} \langle C | V_{12} | C \rangle. \quad (21)$$

The normalization of the AGP wavefunction imposes a relationship between the coefficients  $h_i$  and the occupation numbers  $n_i$  via the condition [32]

$$h_i = \pm \sqrt{n_i(1 - n_i)}. \quad (22)$$

Note that for Coulomb interaction the pair potential  $V_{12}$  is repulsive, so that energy can be gained only through the exchange part  $E_{HF}$  of the Hartree-Fock functional. It can be shown that the amplitudes  $h_i$ 's then must change sign at the "pseudo-Fermi surface" corresponding to the Hartree-Fock solution (i.e. the solution that neglects the term  $E_{BCS}$ ) [32]. The energy can also be gained of course through the term  $E_{BCS}$  in Eq. (20) by the introduction of lattice dynamics as is the case at the superconducting transition [40].

Recently, Goedecker and Umrigar [41,42] have considered an approximation to the two-particle density matrix  $\sigma$  which leads to a functional of natural orbitals similar to form

(20) discussed here. However Csányi and Arias [43] have shown that the electronic states predicted by Ref. [41] are overcorrelated; the reason is that  $\sigma$  is varied over too large a class of functions without the restriction of  $N$ -representability. This problem is circumvented in our case since the the AGP functional is  $N$ -representable by construction.

## V. A SIMPLE IMPLEMENTATION OF THE AGP MODEL

Our main goal is to gain a handle on the nature of occupation numbers in the correlated electron gas. In this spirit, we start by approximating the natural orbitals  $\psi_i$  by the Kohn-Sham orbitals [44] for the one-particle crystal potential; the associated eigenvalues are denoted by  $\varepsilon_i$  with  $\varepsilon_i = 0$  defining the Fermi level following the usual convention.

The solution to the BCS problem involves an energy scale  $\Delta_i$  [29] which determines the mixing of states above and below the Fermi level. The occupation numbers are given by

$$n_i = \frac{1}{2} \left( 1 - \frac{\varepsilon_i}{\sqrt{\varepsilon_i^2 + \Delta_i^2}} \right). \quad (23)$$

$n_i$  is obviously greater than 1/2 for  $\varepsilon_i < 0$ , and less than 1/2 for  $\varepsilon_i > 0$ ; for  $\varepsilon_i \ll \Delta_i$ ,  $n_i \rightarrow 1$  and for  $\varepsilon_i \gg \Delta_i$ ,  $n_i \rightarrow 0$ . At  $\varepsilon_i = 0$ ,  $n_i = 1/2$ . In order to make progress at this point we require a method for estimating the value of  $\Delta_i$ . As already noted, there will be cancellation between the terms  $E_{BCS}$  and  $E_{HF}$  in Eq. (20), and we would physically expect the total energy of the AGP wavefunction to be quite close to that of the Kohn-Sham Hamiltonian. With this motivation, we make the assumption that *the energy cost of electron pairing will, in fact, be roughly compensated by the exchange energy*. If so, it readily follows that

$$|\Delta_i| \sim I_i, \quad (24)$$

where

$$I_i = \left| \int d^3\mathbf{r}_1 d^3\mathbf{r}_2 \frac{\delta^2 E_x}{\delta n(\mathbf{r}_1) \delta n(\mathbf{r}_2)} |\psi_i^*(\mathbf{r}_1) \psi_i(\mathbf{r}_2)|^2 \right| \quad (25)$$

is an exchange type integral [45]. We emphasize that the validity of assumptions leading to Eq. (24) is unclear and that this point deserves further investigation. Within the LDA, an explicit formula for  $I_i$  can be obtained straightforwardly:

$$I_i = \frac{1}{3} \int d^3\mathbf{r} |\psi_i(\mathbf{r})|^4 \frac{v_x(\mathbf{r})}{n(\mathbf{r})} , \quad (26)$$

where  $v_x(\mathbf{r}) = 2/\pi(3\pi^2n(\mathbf{r}))^{1/3}$  is the Kohn-Sham exchange potential [44]. As expected,  $I_i$  is large when  $\psi_i(\mathbf{r})$  is confined to a small spatial region. Finally, the  $n_i$ 's are renormalized in order to satisfy the correct sum rule, i.e.

$$N = \sum_i n_i . \quad (27)$$

The evaluation of the EMD follows along the lines of the standard IPM computations, except that the occupation numbers for the correlated electron gas given by Eq. (23) are used. For the specific EMD and Compton profile results on Li, Be and Al reported in Section VI below, we have used orbitals  $\psi_i$  calculated using linear muffin-tin orbital (LMTO) [46,47] band structure method for convenience, including corrections to the EMD due to the overlapping sphere geometry [48].

The essential parameter which controls the correlation effect in our theory is,

$$\alpha = \Delta/w \sim I_i/w, \quad (28)$$

where  $w$  denotes the relevant valence electron band-width. By keeping Eqs. (23) and (24) in mind, it is evident that when  $I_i$  is comparable to  $w$ ,  $\alpha \sim 1$ , and states deep in the Fermi sea are renormalized inducing significant shift of spectral weight from below to above  $\varepsilon_i = 0$ . On the other hand, when  $I_i \ll w$ ,  $\alpha$  is small and only states near the Fermi momentum are redistributed.

Eq. (26) shows that when  $\psi_i$ 's are the Bloch wavefunctions  $\psi_{\mu\mathbf{k}}$ , then the  $I_i$ 's and hence the  $\Delta_i$ 's will be energy and  $\mathbf{k}$ -dependent, and the resulting correlation correction to the EMD will in general be *anisotropic*. Concerning the break at the Fermi momentum, solutions for some purely repulsive model interactions indicate that  $\Delta_\mu(\mathbf{k})$  can oscillate as a function of energy, and become antisymmetric with respect  $\varepsilon_i$ , going to zero at the Fermi level. [49] If so, the present scheme admits the presence of discontinuities at the Fermi momentum in the EMD. Notably, the AGP satisfies the translational-symmetry requirement of Eq. (6).

## VI. ILLUSTRATIVE RESULTS ON Li, Be AND Al

In this section, we briefly discuss some of the salient features of the EMD predicted by the relatively simple theoretical model of the preceding subsection. Examples of Li, Be and Al are considered as a means of getting a handle on correlation effects for a range of electron concentrations—varying from one electron per atom in Li to two in Be and three in Al. As emphasized already in the introduction, our main purpose here is to establish that the present scheme is capable of explaining, at least in principle, some of the key experimental observations in Li, Be and Al [1–10].

In connection with the Compton spectra, it should be noted that the Compton profile (CP),  $J(p_z)$ , represents the double integral of the ground-state EMD  $\rho(\mathbf{p})$ :

$$J(p_z) = \iint \rho(\mathbf{p}) dp_x dp_y, \quad (29)$$

where  $p_z$  lies along the scattering vector of the x-rays.

Li is considered first. Using Eq. (26), we obtain  $I_i \approx 0.1$  Ry, which when compared with the valence electron band width,  $w \approx 0.25$  Ry, yields  $\alpha \sim I_i/w = 0.4$ . This implies that the IPM values of occupation numbers will be modified substantially by correlations. Fig. 2 compares a typical CP (results along [100] are given) in Li for LDA with and without the LP correction, and the AGP model computation. The LDA (solid) displays a cusp around 0.6 a.u. which reflects the break in the EMD at  $p_F$ . The addition of the LP correction (light dashed) shifts some spectral weight from low to high momenta, but the cusp at  $p_F$  is essentially unchanged. In sharp contrast, in the AGP curve (thick dashed), the feature at  $p_F$  is completely smoothed out and the EMD is redistributed throughout the momentum space. The AGP results are at least qualitatively similar to the behavior of the experimental CP's in Li which show that the size of the discontinuity  $Z_k$  at  $p_F$  is very small and that the measured CP is substantially lower than LDA around  $\mathbf{p} = 0$  [1–4]. We should keep in mind nevertheless the fact that the AGP results in Fig. 2 invoke a series of approximations which might oversmooth the discontinuity at  $p_F$ . Notably, spin-polarized electronic structure

computations indicate the importance of spin-wave fluctuations in Li [50], suggesting that some renormalization of the occupation numbers in Li could also be produced by such a mechanism.

Interestingly, an extensive study of  $\text{Li}_{100-x}\text{Mg}_x$  disordered alloys [3] over the composition range  $0 \leq x \leq 40$  indicates that the measured CP's come into better accord with the LDA predictions with increasing Mg concentration. This observation will find a natural explanation in our theoretical framework since we expect the width of the valence band to increase with increasing Mg content with little change in the exchange integral  $I_i$ , so that the parameter  $\alpha$  (see, Eq. 28) will presumably decrease as will the correlation effect.

Turning to Be, the exchange integral is computed to be,  $I_i \approx 0.1$  Ry, but  $w \approx 0.8$  Ry, giving  $\alpha \approx 0.13$ . Therefore the correlation effect on the EMD in Be is smaller than Li, consistent with experimental observations [5–7]. Fig. 3 focuses on the difference,  $\Delta J^{Theory} = J_{AGP} - J_{LDA}$ , between the AGP and the LDA (including the LP correction) predictions of CP's along two different crystal directions. The LP correction (dashed) is seen to mimic the overall shape of  $\Delta J^{Theory}$ . However, in contrast to the LP correction which is *isotropic*, the residual correlation correction given by  $\Delta J^{Theory}$  is *anisotropic*. Along [100],  $\Delta J^{Theory}$  differs relatively little from the LP curve, but along [001] the excursions are much larger. The results of Fig. 3 are in qualitative accord with some of the characteristics of the experimental CP's in Be. By comparing the residuals of our Fig. 3 with the experimental residuals (defined as,  $\Delta J^{Expt} = J_{Expt} - J_{LDA}$ , which are given in Fig. 4 of Ref. [7]), it will be seen that  $\Delta J^{Expt}$ , like  $\Delta J^{Theory}$ , deviates little from the LP curve along [100]; in sharp contrast, along [001]  $\Delta J^{Expt}$  contains a remarkable pattern of undulations rather similar to that seen in  $\Delta J^{Theory}$  in Fig. 3. Further study is needed to pin down the origin of specific structures in  $\Delta J^{Theory}$  in terms, for example, of the Fermi surface features.

Finally, in the case of Al, we find  $I_i \approx 0.05$  Ry, which as expected is small, reflecting the decrease of  $I_i$  with increasing electron density. On the other hand, the band width  $w \approx 1$  Ry is quite large, so that  $\alpha \approx 0.05$  is rather small. Therefore, the EMD in Al will not suffer much redistribution beyond the LDA via electron correlations. This again is consistent with

experimental observations which show that the EMD in Al is described reasonably well by the conventional LDA picture [8–10]. We illustrate this point further by Fig. 3 where the LDA and AGP momentum densities  $\rho(p)$  are compared along a typical direction (note these are 3D momentum densities and not the CP’s). The AGP and LDA are seen to be quite close overall, some rounding of the Fermi break in AGP notwithstanding.

## VII. SUMMARY AND CONCLUSIONS

We discuss the theoretical treatment of the EMD in the correlated electron gas with the purpose of developing an understanding of recent high resolution Compton scattering experiments on a variety of materials. EMD can be expressed rigorously in terms of the eigenfunctions and eigenvalues of the one-particle density matrix, which play the roles of effective orbitals  $\psi_i$ ’s – the ‘natural orbitals’, and the associated occupation numbers  $n_i$ ’s, respectively. Much of the existing EMD work in crystals is based on the use of Bloch wavefunctions computed within the LDA and the related IPM values of occupation numbers (i.e., 1 for filled and 0 for empty states). In the DFT, the expectation value of any operator (excepting the electron density  $n(\mathbf{r})$ ) must be corrected with respect to its IPM value in order to include the effect of correlations in the interacting system. The standard calculation of such an LP correction to the IPM momentum density involves the momentum density  $\rho_h(p)$  in the interacting HEG. Although many attempts to evaluate  $\rho_h$  in the HEG have been made, the recent QMC results are perhaps the most accurate. In this connection, we provide a convenient parametrization of the QMC data for  $\rho_h$  as a function of the electron density parameter  $r_s$ ; this form of  $\rho_h$  should be used for computing the LP correction. Note that the LDA-based LP correction possesses fundamental limitations, e.g., it can only describe an isotropic redistribution of the EMD.

In order to go beyond the framework of the DFT, we propose using a BCS-like wavefunction in which the starting point is an electron singlet pair or a ‘geminal’, and the many body wavefunction is constructed as an AGP. Although such an approach has been invoked

previously in a variety of problems, we are not aware of its application to treat the EMD in extended systems. The AGP wavefunction tends to minimize the effects of the exclusion principle and possesses a fundamentally different nodal structure compared to the Slater-Jastrow type many body wavefunctions based on single-particle orbitals which are implicit in the LDA and QMC work. We begin to explore the nature of the EMD in the AGP scheme in this article by approximating the natural orbitals by the Kohn-Sham orbitals. By making the assumption that the energy gained through the BCS-like term will be roughly compensated by the exchange-correlation part of the Hartree-Fock term in the total energy functional, we show that the BCS energy scale,  $\Delta_i \sim I_i$ , where  $I_i$  is a readily computed exchange-type integral. The key parameter which controls the redistribution of states in our theory then is,  $\alpha \sim I_i/w$ , with  $w$  being the valence electron band-width.

Finally, we consider the application of the AGP method to discuss the EMD and Compton spectra of Li, Be and Al as illustrative examples. In Li, we find  $\alpha \sim 0.4$ , implying a substantial renormalization of the LDA states, in essential accord with experimental results which indicate the break in the EMD to be renormalized to a nearly zero value. In Be,  $\alpha \sim 0.13$ , and the theory predicts *anisotropic* correlation effects in the EMD which show a remarkable resemblance to the anisotropy of measured Compton profiles. In Al, we estimate,  $\alpha \sim 0.05$ , so that the correlations yield relatively little modification of the EMD, and here again, this is consistent with the experimental observations which indicate that Al is described reasonably within the conventional LDA picture. Taken together, these results—involving a range of electron concentrations, show the potential of the AGP method in providing a theoretical method for describing correlation effects on the EMD in wide classes of materials, although further work is necessary in this connection. Other open questions concern the excitation properties of the AGP ground state.



## ACKNOWLEDGMENTS

This work is supported by the US Department of Energy under contract W-31-109-ENG-38 and benefited from the allocation of supercomputer time at the NERSC and the Northeastern University Advanced Scientific Computation Center (NU-ASCC).

## REFERENCES

- [1] Y. Sakurai, Y. Tanaka, A. Bansil, S. Kaprzyk, A.T. Stewart, Y. Nagashima, T. Hyodo, S. Nanao, H. Kawata, and N. Shiotani, Phys. Rev. Lett. **74**, 2252 (1995).
- [2] W. Schülke, G. Stutz, F. Wohler, and A. Kaprolat, Phys. Rev. B **54**, 14381 (1996).
- [3] G. Stutz, F. Wohler, A. Kaprolat, W. Schülke, Y. Sakurai, Y. Tanaka, M. Ito, H. Kawata, N. Shiotani, S. Kaprzyk, and A. Bansil, Phys. Rev. B **60**, 7099 (1999).
- [4] Y. Tanaka, Y. Sakurai, A.T. Stewart, N. Shiotani, P.E. Mijnders, S. Kaprzyk, and A. Bansil, Phys. Rev. B **63**, 45120 (2001).
- [5] K. Hämäläinen, S. Manninen, C.-C. Kao, W. Caliebe, J.B. Hastings, A. Bansil, S. Kaprzyk, and P.M. Platzman, Phys. Rev. B **54**, 5453 (1996).
- [6] M. Itou, Y. Sakurai, T. Ohata, A. Bansil, S. Kaprzyk, Y. Tanaka, H. Kawata, and N. Shiotani, J. Phys. Chem. Solids **59**, 99 (1998).
- [7] S. Huotari, K. Hämäläinen, S. Manninen, S. Kaprzyk, A. Bansil, W. Caliebe, T. Buslaps, V. Honkimäki, and P. Suortti, Phys. Rev. B **62**, 7956 (2000).
- [8] P. Suortti, T. Buslaps, V. Honkimäki, C. Metz, A. Shukla, Th. Tschentscher, J. Kwiatkowska, F. Maniowski, A. Bansil, S. Kaprzyk, A.S. Kheifets, D.R. Lun, T. Sattler, J.R. Schneider, and F. Bell, J. Phys. Chem. Solids **61**, 397 (2000).
- [9] T. Ohata, M. Itou, I. Matsumoto, Y. Sakurai, H. Kawata, N. Shiotani, S. Kaprzyk, P.E. Mijnders, and A. Bansil, Phys. Rev. B **62**, 16528 (2000).
- [10] I. Matsumoto, J. Kwiatkowska, F. Maniowski, A. Bansil, S. Kaprzyk, M. Itou, H. Kawata, and N. Shiotani, J. Phys. Chem. Solids **61**, 375 (2000).
- [11] Y. Sakurai, S. Kaprzyk, A. Bansil, Y. Tanaka, G. Stutz, H. Kawata, and N. Shiotani, J. Phys. Chem. Solids **60**, 905 (1999).
- [12] E. Daniel and S.H. Vosko, Phys. Rev. **120**, 2041 (1960).

- [13] B.I. Lundqvist, Phys. Kondens. Materie **6**, 206 (1967).
- [14] A.W. Overhauser, Phys. Rev. B **3**, 1888 (1971).
- [15] L.J. Lantto, Phys. Rev. B **22**, 1380 (1980).
- [16] B. Farid, B. Heine, G. Engel, and I. Robertson, Phys. Rev. B **48**, 11602 (1993).
- [17] G. Ortiz and P. Ballone, Phys. Rev. B **50**, 1391 (1994).
- [18] L. Lam and P.M. Platzman, Phys. Rev. B **9**, 5122 (1974).
- [19] G.E.W. Bauer, Phys. Rev. B **27**, 5912 (1983).
- [20] D.A. Cardwell and M.J. Cooper, J. Phys. Condens. Matter **1**, 9357 (1989).
- [21] Y. Kubo, J. Phys. Soc. Jpn. **65**, 16 (1996).
- [22] W. Shülke, J. Phys. Soc. Jpn. **68**, 2470 (1999).
- [23] A.G. Eguiluz, W. Ku, and J.M. Sullivan, J. Phys. Chem. Solids **61**, 383 (2000).
- [24] B. Kralik, P. Delaney, and S.G. Louie, Phys. Rev. Lett. **80**, 4253 (1998).
- [25] C. Filippi and D.M. Ceperley, Phys. Rev. B **59**, 7907 (1999).
- [26] P. Fulde, *Electron Correlations in Molecules and Solids* (Springer, Berlin, 1995).
- [27] R.O. Jones and O. Gunnarsson, Rev. Mod. Phys **61**, 689 (1989).
- [28] J.M. Blatt, Progress of Theor. Phys. **27**, 1137 (1962).
- [29] J. M. Blatt, *Theory of Superconductivity* (Academic Press, New York 1964).
- [30] G. Bessis, P. Espanat and S. Bratoz, Int. J. Quantum Chem. **3**, 205 (1969).
- [31] J.P. Bouchard and C. Lhuillier, Z. Phys. B **75**, 283 (1989)
- [32] O. Goscinski, Int. J. Quantum Chem. Quantum Chem. Symp **16**, 591 (1982).
- [33] B. Barbiellini, J. Phys. Chem. Solids **61**, 341 (2000).

- [34] A.J. Coleman, Rev. Mod. Phys. **35**, 668 (1963).
- [35] P.O. Löwdin, Phys. Rev. **97**, 1474 (1955).
- [36] O. Goscinski and P. Lindner, J. Math. Phys **11**, 1313 (1970).
- [37] W. Kohn, Phys. Rev. Lett. **76**, 3168 (1996).
- [38] Y. Yasuhara and Y. Kawazoe, Physica **85A**, 416 (1976).
- [39] Overhauser, Can. J. Phys **73**, 683 (1995).
- [40] M. Weger, B. Barbiellini and M. Peter, Z. Phys. B **94**, 387 (1994).
- [41] S. Goedecker and C. J. Umrigar, Phys. Rev. Lett. **81**, 866 (1998).
- [42] S. Goedecker and C. J. Umrigar in *Many-electron densities and reduced density matrices*, edited by J. Cioslowski and A. Szarecka (Kluwer Academic, Dordrecht, 2000).
- [43] G. Csányi and T. A. Arias, Phys. Rev. B **61**, 7348 (2000).
- [44] W. Kohn and L.J. Sham, Phys. Rev. **140** A, 1133 (1965).
- [45] J.F. Janak, Phys. Rev. B **16**, 255 (1977).
- [46] O.K. Andersen, Phys. Rev. B **12**, 3060 (1975).
- [47] T. Jarlborg and G. Arbman, J. Phys. F **7**, 1635 (1977).
- [48] A.K. Singh and T. Jarlborg, J. Phys. F **15**, 727 (1985).
- [49] B. Barbiellini, M. Weger and M. Peter, Helvetica Phys. Acta **66**, 842 (1993).
- [50] T. Jarlborg, Physica Scripta **37**, 795 (1988).

## Figure Captions

FIG. 1. Momentum density  $\rho(p)$  in the homogeneous electron gas. The momentum  $p$  is given in scaled units of the free electron Fermi momentum  $p_F$ . Parameterized QMC (solid) and LDA (dashed) results are shown for  $r_s$  values of 2 and 5, as discussed in the text.

FIG. 2. Theoretical results for the [100] Compton profile in Li are compared for three different models: LDA without LP correction (solid), LDA with LP correction (light dashed), and the AGP scheme discussed in the text (heavy dashed).

FIG. 3. Effect of correlation on the Compton profile along two different directions in Be. The solid curve gives the residual difference,  $\Delta J^{Theory} = J_{AGP} - J_{LDA}$ , between the LDA and the AGP profiles; note, that  $J_{LDA}$  here includes the Lam-Platzman correction, which is also shown separately (dashed lines) for reference.

FIG. 4. 3D momentum density along [110] is compared in Al for the LDA and the AGP case.

# FIGURES

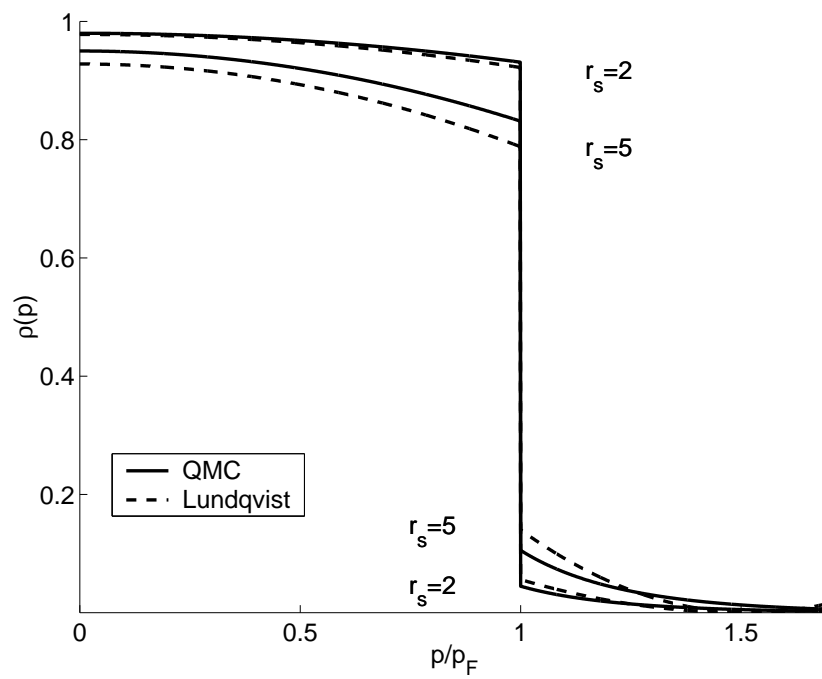


FIG. 1.

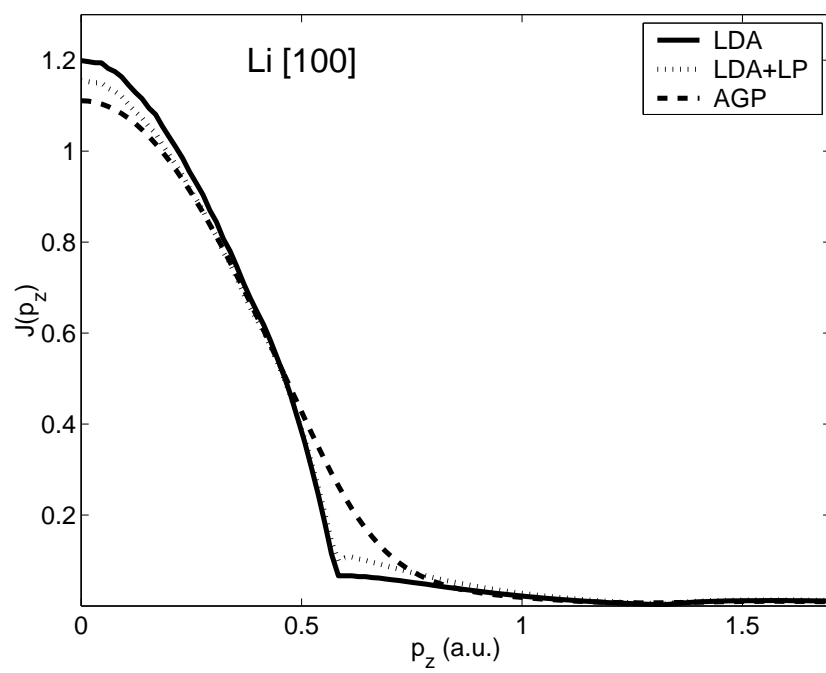


FIG. 2.

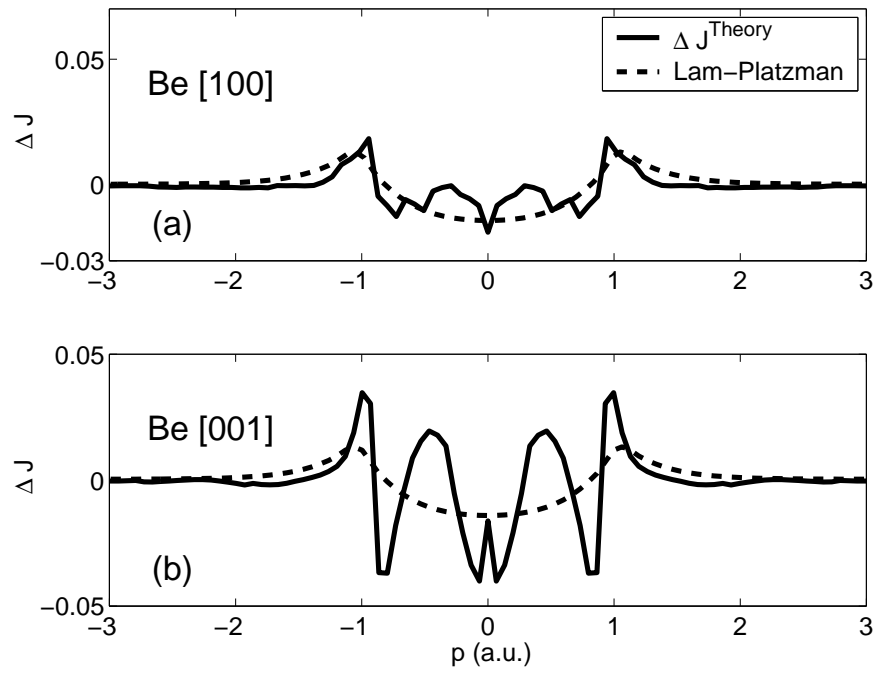


FIG. 3.



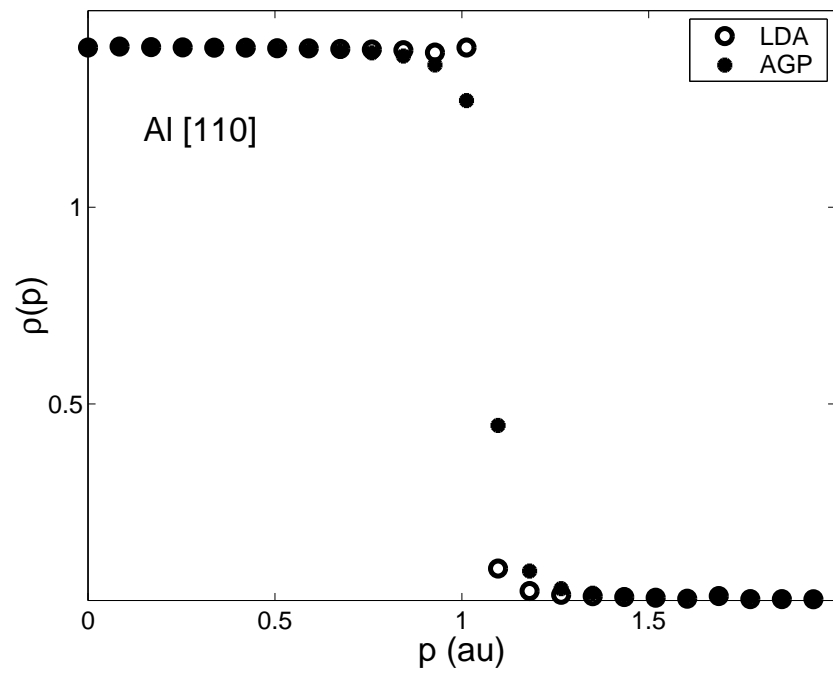


FIG. 4.